

Quantitative monitoring of relative clock wander between signal and sampling sources in asynchronous optical under-sampling system

Huixing Zhang (张慧星)^{1,2*} and Wei Zhao (赵卫)¹

¹State Key Laboratory of Transient Optics and Photonics, Xi'an Institute of Optics and Precision Mechanics, Chinese Academy of Sciences, Xi'an 710119, China

²Graduate University of Chinese Academy of Sciences, Beijing 100049, China

*Corresponding author: huixingde@hotmail.com

Received April 29, 2011; accepted August 25, 2011; posted online October 18, 2011

Optical performance monitoring using asynchronous optical or electrical sampling has gained considerable attention. Relative clock wander between data signal and sampling source is a typical occurrence in such systems. A method for the quantitative monitoring of the relative clock wander in asynchronous optical under-sampling system is presented. With a series of simulations, the clock wanders recovered using this method are in good agreement with the preset clock wanders of different amounts and frequencies for both RZ and NRZ signals. Hence, the reliability and robustness of the method are proven.

OCIS codes: 060.0060, 060.4510.

doi: 10.3788/COL201210.030601.

With the growing demand for the ultra-high capacity fiber-optic networks, a straightforward opto-electric conversion in the receiver end is far from sufficient to meet the high bandwidth required in such systems. Optical sampling technique^[1–5] enables prior sampling of the signal in the optical domain before photo detection, significantly degrading the bandwidth requirement for the photo detectors. To control the timing of the sampling event, synchronous optical sampling system^[6–8] with optical clock recovery is implemented. However, this is impractical in terms of technical realization and deployment cost. Thus, asynchronous optical^[9,10] and electrical sampling^[11] have become the focus in recent years due to their reduced hardware complexity. And they both do not require optical or electrical clock recovery. Recently, up to 500-Gb/s eye diagram monitoring has been achieved using asynchronous all optical sampling^[12]. However, it yields a random clock wander between the signal and sampling sources in such system because no clock recovery is applied. Monitoring of the relative clock wander is very useful in obtaining further insight into the asynchronous sampling system and especially in choosing the proper sampling source for certain data source under testing (the smaller the relative wander, the more the system performance is optimized). However, literature on the observation of the relative clock wander in asynchronous sampling system is insufficient.

In this letter, a method for quantitatively observing clock wander in asynchronous under-sampling system is demonstrated by validating the reliability and the robustness with a series of numerical simulations on both return-to-zero (RZ) and nonreturn-to-zero (NRZ) signals. The method for monitoring the relative clock wander in asynchronous sampling system is described. The mimic sampling experiments on NRZ and RZ signals by means of simulations to verify the clock-wander observation method in terms of reliability and robustness are

presented.

The schematic illustration comparing the under-sampling process of the asynchronous and synchronous sampling systems is depicted in Fig. 1. It shows the first six sampling events perform in the system. As shown on the plot, S is the under sampling ratio (the nearest integer number of the ratio between the signal bit rate and the sampling frequency). Black dots indicate the wander-free synchronous sampling, and the sampling interval is denoted as T'_s . It should be noted that T'_s is in scale of the signal bit period T_b . The red dots denote the asynchronous sampling affected by the relative clock drift δ_n where n starts counting from 0, corresponding to the time index of the samples. If δ_n is known, the plot of the clock wander can be given, as shown in Fig. 2.

Figure 1 shows that the relative clock drift δ_n can be obtained by using the timing of the samples in asynchronous sampling to subtract the timing of the corresponding samples in synchronous sampling. Accordingly, $\delta_1 = t_1 - T'_s$, as shown in Fig. 1, can be written more generally as $t_n = nT'_s + \delta_n$, where t_n signifies the timing of the samples in asynchronous sampling. It suggests that the clock wander can be acquired straightforwardly by subtracting the linear drift from t_n . In this case, we apply a sliding window finite impulse response (FIR) filter with $2K + 1$ taps to obtain the timing of each sample as^[12]

$$Y_n = \sum_{k=-K}^K c_n y_{n+k}. \quad (1)$$

Subsequently, the tap coefficients c_n are given by

$$c_n = W_n \cdot e^{-i2n\pi f_a} \quad (n = -K, \dots, K), \quad (2)$$

where W_n is a windowing function and f_a is the aliased frequency which can be found from an averaging periodogram (over M blocks wherein each block contains L samples) of the transformed samples y_n , i.e., after

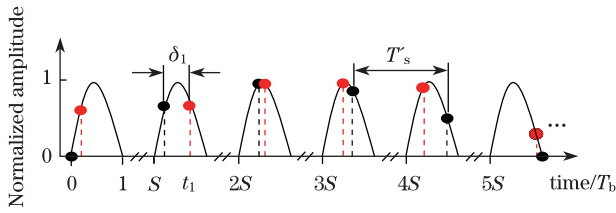


Fig. 1. (Color online) Schematic illustration of the comparison between synchronous sampling process and asynchronous sampling process.

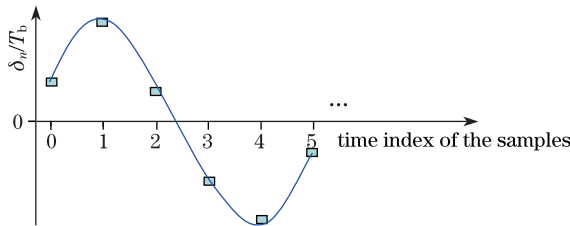


Fig. 2. Relative clock wander δ_n .

a nonlinear function $f(x)$ has been applied to the normalized samples. The nonlinear function $f(x)$ emphasizes the transition between the two levels (corresponding to 0 and 1 in the transmitted sequence)^[11]. Figure 3 shows an example of the averaging periodogram. The highest peak, denoted as the aliased frequency, manifests itself when excluding the 0 frequency component. It is worth mentioning that the positive or negative aliased frequency only decides the reconstruction direction and leads a mirror eye with each other.

For FIR filter of $2K + 1$ taps, t_n is given as

$$t_n = \frac{\arg Y_n}{2\pi} \quad (3)$$

Based on this, we can obtain the clock wander directly by subtracting the linear drift.

It should be noted that this clock-wander observing method is independent of the signal bit rate and can be applied to any data format. Moreover, any under-sampling system, including electrical or all-optical sampling as well as linear or nonlinear implementation, can be used for data acquisition.

The sampling processes on RZ and NRZ signals of pseudo-random binary sequence (PRBS) are numerically simulated by using the popular software package LabVIEW to investigate the reliability and robustness of this clock-wander observing method. In the simulation, the data pulse simulated is of Gaussian-type shape^[13]

$$u(0, t) = \exp\left[-\frac{1}{2}\left(\frac{t}{T_0}\right)^{2m}\right], \quad (4)$$

where parameter m controls the degree of edge sharpness. T_0 is the half width (at $1/e$ -intensity point) given by

$$T_0 = \frac{T_{FWHM}}{2(\ln 2)^{\frac{1}{2m}}}, \quad (5)$$

where T_{FWHM} indicates the full-width at half-maximum of the pulse.

For the sampling of the RZ signal, RZ data pulse is given by $m = 1$ (Gaussian). In our simulation, bit period of the signal $T_b = 0.2873$ s and sampling period $T_s = 1$ s are adopted to ensure that the time step is an irrational number. Otherwise, only particular points of the bit slot can be sampled. The under-sampling ratio S is chosen to be 3. T_{FWHM} is set at 25% of T_b , which leads to $T_0 = 0.043$. The extinction ratio of the pulse is -15 dB. PRBS with a pattern length of $2^7 - 1$ is used and 8×10^4 samples are taken. The clock wander δ_n is modeled as the form of sinusoidal signal for convenience. Hence, the preset sampling timing t'_n of the samples can be calculated accordingly by the expression mentioned before. For simplicity, no additive timing jitter is launched to the signal. Sinusoidal-like clock wanders of different frequencies and amplitudes are imparted to examine the reliability of the method for RZ signal. The comparison of the clock wander recovered at the receiver end with the one preset at the transmitter end is simultaneously obtained. Figure 4(a) shows the clock wander recovered in comparison with the preset clock wander as a sinusoidal signal with an amplitude of 10% of T_b and only one

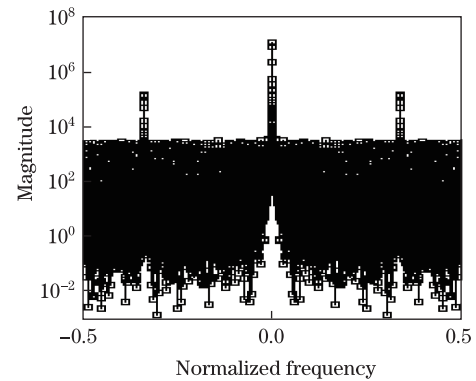


Fig. 3. Example of periodogram with frequency normalized to the sampling frequency.

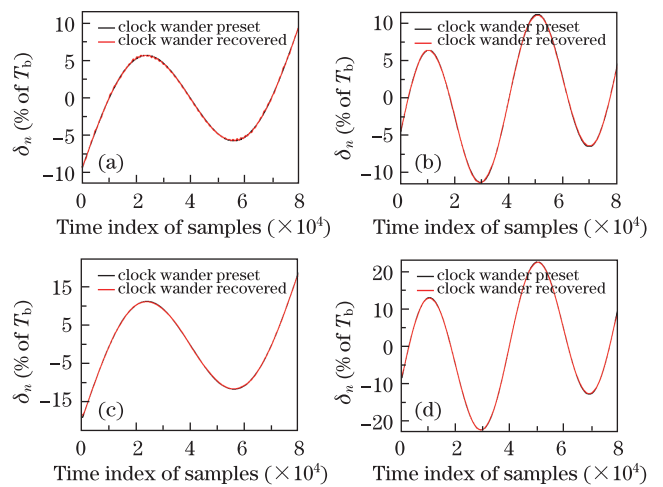


Fig. 4. Recovered clock wander for RZ signal in comparison with preset clock wander of a sinusoidal signal over 8×10^4 samples. (a) Clock wander preset with amplitude of 10% repeats 1 cycle; (b) clock wander preset with amplitude of 10% repeats 2 cycles; (c) clock wander preset with amplitude of 20% repeats 1 cycle; (d) clock wander preset with amplitude of 20% repeats 2 cycles.

cycle repetition over the whole sample-set. Figure 4(b) shows the case of presetting clock wander with the same amplitude but a double frequency in testing the robustness of the method. In Figs. 4(c) and (d), the amplitudes of the preset clock wanders are raised to 20% of T_b . From the plots, a good agreement can be seen clearly between the recovered clock wander and the corresponding preset clock wander. The slight distortion of the recovered clock wander is due to the limited precision of the built-in Labview program of the linear fit, where the slope calculated slightly deviates from the true value. To clarify the comparison, the preset clock wander shown as a black line in Fig. 4 is not the original sinusoidal signal added but the one obtained at the transmitter end by subtracting linear fit from the preset timing of the samples.

For the sampling of NRZ signal, NRZ data pulse is given by $m = 4$ (super-Gaussian). Time period of the signal $T_b = 0.2873$, $T_s = 1$ s, and the under-sampling ratio S is 3. With T_{FWHM} equal to bit duration for NRZ signal, we obtained $T_0 = 0.150$. Other simulation conditions implemented in simulations on RZ signal are adopted for consistency. Results of the clock wander recovered which are fairly consistent with those of the preset clock wander are shown in Fig. 5.

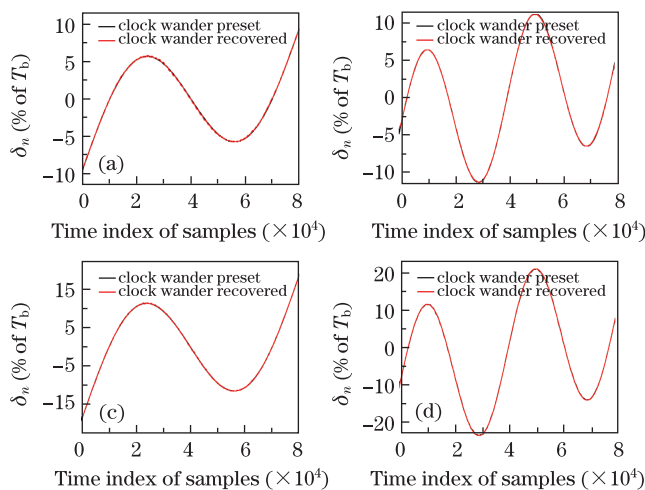


Fig. 5. Recovered clock wander for NRZ signal in comparison with preset clock wander of a sinusoidal signal over 8×10^4 samples. (a) Clock wander preset with amplitude of 10% repeats 1 cycle; (b) clock wander preset with amplitude of 10% repeats 2 cycles; (c) clock wander preset with amplitude of 20% repeats 1 cycle; (d) clock wander preset with amplitude of 20% repeats 2 cycles.

In conclusion, we present a quantitative monitoring method for the relative clock wander between signal and sampling sources in asynchronous under-sampling system. The quality of the method is verified in terms of its reliability and robustness through a series of sampling simulations on both RZ and NRZ signals. At the transmitter end, clock wander preset, as a sinusoidal signal, varies with respect to amplitude or frequency. Subsequently, such clock wander is recovered correspondingly at the receiver end. The preset and the recovered clock wanders are in good agreement, validating the reliability and robustness of the clock-wander observing method.

The authors would like to thank Carsten Schmidt-Langhorst for the fruitful discussions and the Chinese Academy of Sciences-German Academic Exchange Service (DAAD) joint scholarship for the financial support.

References

1. C. Dorrer, C. R. Doerr, I. Kang, R. Ryf, J. Leuthold, and P. J. Winzer, *J. Lightwave Technol.* **23**, 178 (2005).
2. S. Diez, R. Ludwig, C. Schmidt, U. Feiste, and H. G. Weber, *IEEE Photon. Technol. Lett.* **11**, 1402 (1999).
3. S. Kawanishi, T. Yamamoto, M. Nakawawa, and M. M. Fejer, *Electron. Lett.* **37**, 842 (2001).
4. J. Li, J. Hansryd, P. O. Hedekvist, P. A. Andrekson, and S. N. Knudsen, *IEEE Photon. Technol. Lett.* **13**, 987 (2001).
5. S. Nogiwa, H. Ohta, Y. Kawaguchi, and Y. Endo, *Electron. Lett.* **35**, 917 (1999).
6. C. Schmidt-Langhorst and H.-G. Weber, *J. Opt. Fiber Commun. Rep.* **2**, 86 (2005).
7. M. Shirane, Y. Hashimoto, H. Yamada, and H. Yokoyama, *IEICE Trans. Electron.* **E87-C**, 1173 (2004).
8. N. Yamada, S. Nogiwa, and H. Ohta, *IEEE Photon. Technol. Lett.* **16**, 1125 (2004).
9. D. Tang, J. Zhang, Y. Liu, and W. Zhao, *Chin. Opt. Lett.* **8**, 630 (2010).
10. M. Westlund, H. Sunnerud, M. Karlsson, and P. A. Andrekson, *J. Lightw. Technol.* **23**, 1088 (2005).
11. G. Moustakides, F. Cerou, O. Audouin, and L. Noirie, in *Proceedings of 11th European Signal Processing Conference* 375 (2002).
12. J. Li, M. Westlund, H. Sunnerud, B.-E. Olsson, M. Karlsson, and P. Andrekson, *IEEE Photon. Technol. Lett.* **16**, 566 (2004).
13. G. P. Agrawal, *“Nonlinear Fiber Optics”* (Academic Press Inc., San Diego, 1995) chap.3.